Acta Pharmacologica Sinica (2013) 34: 1437–1448

www.nature.com/aps

Original Article

Pharmacokinetic evaluation of the anticancer prodrug simmitecan in different experimental animals

Zhe-yi HU#, Xiu-xue LI#, Fei-fei DU, Jun-ling YANG, Wei NIU, Fang XU, Feng-qing WANG, Chuan LI, Yan SUN*

Centre for Drug Metabolism and Pharmacokinetics Research, Shanghai Institute of Materia Medica, Chinese Academy of Sciences, Shanghai 201203, China

Aim: To investigate the pharmacokinetics and disposition of simmitecan (L-P) that was a water-soluble ester prodrug of chimmitecan (L-2-Z) with potent anti-tumor activities in different experimental animals, and to assess its drug-drug interaction potential.
Methods: SD rats were injected with a single iv bolus doses of L-P (3.75, 7.5 and 15 mg/kg). The pharmacokinetics, tissue distribution, excretion and metabolism of L-P and its active metabolite L-2-Z were studied through quantitative measurements and metabolite profiling with LC/MS. The binding of L-P and L-2-Z to rat plasma proteins was examined using an ultrafiltration method. Systemic exposures of beagle dogs to L-P as well as drug distribution in tumors of the nude mice xenograft model of human hepatic cancer SMMC-7721 cells were also examined. The metabolism of L-P by liver mcirosomal carboxylesterase *in vitro* was investigated in different species. The effects of L-P and L-2-Z on cytochrome P450 enzymes were examined using commercial screening kits.
Results: The *in vivo* biotransformation of L-P to L-2-Z showed a significant species difference, with a mean elimination half-life t1/2 of approximately 1.4 h in rats and 1.9 h in dogs. The systemic exposure levels of L-P and L-2-Z were increased in a dose-dependent manner. In rats, approximately 66% of L-P and 79% of L-2-Z were bound to plasma proteins. In rats and the nude mice bearing human hepatic cancers, most organ tissues had significantly higher concentrations of L-P than the corresponding plasma levels. In the tumor tissues, the L-P levels were comparable to those of plasma, whereas the L-2-Z levels were lower than the L-P levels. In rats, L-P was eliminated mainly via biliary excretion, but metabolism played an important role in elimination of the intact L-P. Finally, L-P and L-2-Z exerted moderate inhibition on the activity of CYP3A4 *in vitro*.
Conclusion: L-P and L-2-Z have relatively short elimination half-lives and L-P is mainly eliminated via biliary excretion. The species difference in the conversion of L-P to L-2-Z and potential drug-drug interactions due to inhibition of CYP3A4 should be considered in further studies.

Keywords: pharmacokinetics; distribution; metabolism; excretion; L-P; L-2-Z; carboxylesterase; species difference; prodrug

Acta Pharmacologica Sinica (2013) 34: 1437–1448; doi: 10.1038/aps.2013.74; published online 23 Sep 2013

Introduction

Camptothecin (CPT) derivatives potentially have inhibitory activity on DNA topoisomerase I and are promising compounds in anticancer research. Two CPT derivatives, irinotecan and topotecan, have been approved for clinical use[1, 2]. Chimmitecan (L-2-Z; 9-allyl-10-hydroxy-camptothecin), a novel 9-substituted camptothecin, has improved anticancer potency and pharmacologic profiles, compared to the clinically available CPT analogues[3]. The solubility issue associated with L-2-Z was overcome by the synthesis of simmitecan (L-P; 9-allyl-10-piperidyl piperidine formyloxy-camptothecin). This water-soluble prodrug has a dipiperidyl carbamate at position 10 of the CPT skeleton. This entity is hydrolyzed by carboxylesterases *in vivo* to form the active metabolite, L-2-Z, which possesses strong anticancer activity against a number of different human tumor cell lines *in vitro*. While the IC_{50} of L-2-Z is in the nanomolar range[3], L-P does not show significant antitumor activity. The prodrug modification of L-P is characterized by the utilization of a polar pro-moiety to increase water solubility. This structural design is similar to the design used for irinotecan.

Because L-P was identified as a potential anticancer agent, studies were conducted to characterize the *in vivo* distribution, metabolism, excretion, and pharmacokinetics of L-P (the prodrug) and its active metabolite L-2-Z in rodent and non-

# These authors contributed equally to this work.
* To whom correspondence should be addressed.
E-mail sunyan@mail.shcnc.ac.cn
Received 2013-05-04 Accepted 2013-05-14

rodent experimental animals. In addition, the *in vitro* metabolism for different animal species and the drug-drug interaction potentials were also investigated. Pharmacokinetic studies in animal models are an important component of the clinical development for this agent because they relate preclinical studies to patient treatment. This report presents the results of the disposition and pharmacokinetic studies of L-P and its active metabolite L-2-Z in rats, tumor-bearing nude mice and beagle dogs. In addition, *in vitro* data of L-P and L-2-Z, including the inhibitory effects on cytochrome P450 enzymes and plasma protein binding, are reported here. Recently, L-P has received China Food and Drug Administration new drug approval to be continued its study in a phase I clinical trial (goverment identifier: NCT01832298); this study presents the results of the disposition and pharmacokinetic studies of L-P and L-2-Z obtained from preclinical animal models. The collective information helped in the design of appropriate clinical regimens for investigating this drug in phase I clinical trials.

Materials and methods

Chemicals and reagents

Simmitecan (L-P, 9-allyl-10-piperidyl piperidine formyloxy-camptothecin, hydrochloride form; ≥98%) and chimmitecan (L-2-Z, 9-allyl-10-hydroxy-camptothecin, free base form; ≥98%) were supplied by the Department of Medicinal Chemistry, Shanghai Institute of Materia Medica, Chinese Academy of Sciences (Shanghai, China). Irinotecan (hydrochloride form; ≥98%) and camptothecin (free-base form; ≥98%), which were used as internal standards, were obtained from the National Institute for Food and Drug Control (Beijing, China). *Bis*(4-nitrophenyl) phosphate (BNPP, ≥99%) and taurocholic acid were obtained from Sigma-Aldrich (St Louis, MO, USA). Organic solvents of HPLC-grade and ether were obtained from Sinopharm Chemical Reagent Co, Ltd (Shanghai, China). HPLC-grade water was prepared with a Direct-Q 3 UV water purifying system (Millipore, Bedford, MA, USA). Human liver microsomes and CYP inhibitor screening kits for the rapid identification of *in vitro* inhibitors of CYP1A2, CYP2C9, CYP2C19, CYP2D6, and CYP3A4 were obtained from BD Gentest (Woburn, MA, USA).

Experimental animals

The use and treatment of rats complied with the Guidance for Ethical Treatment of Laboratory Animals (The Ministry of Science and Technology of China, 2006; www.most.gov.cn/fggw/zfwj/zfwj2006). Animal studies were conducted according to the protocols approved by the Institutional Animal Care and Use Committee at the Shanghai Institute of Materia Medica (Shanghai, China). Male and female Sprague-Dawley rats weighing 250–300 g were obtained from the Sino-British SIPPR/BK Laboratory Animal Co, Ltd (Shanghai, China). The rats were housed in rat cages (42 cm×24 cm×24 cm; 3 rats/cage) in a unidirectional airflow room under controlled temperature (20–24 °C), humidity (45%–55%) and a 12-h cycle of light and dark. Filtered tap water was available *ad libitum*. The rats were given commercial rat chow *ad libitum*. Prior to the experiment, rats were acclimatized to the facilities and environment for 7 d. After study use, the rats were euthanized with CO_2 gas.

Male and female nude mice weighing 18–20 g and bearing the human hepatocellular carcinoma SMMC-7721 cell line were obtained from State Key Laboratory of Drug Research, Division of Anti-Tumor Pharmacology, Shanghai Institute of Materia Medica. After study use, the mice were euthanized with CO_2 gas.

Male and female beagle dogs weighing 8.1–10.1 kg were obtained from the Agricultural and Biotech Training Centre, Shanghai Jiao Tong University (Shanghai, China). The dogs were housed under controlled environmental conditions (temperature, 20–24 °C; humidity, 45%–55%; 12-h of light/dark cycle and 8–10 air changes per hour). Dogs were acclimatized to the facilities and environment for 15 d before the experiments.

Rat studies

For plasma pharmacokinetic studies, rats were randomly assigned to three treatment groups and received a single iv bolus dose of L-P at 3.75, 7.5, or 15 mg/kg (administered via the tail vein; 3 mL/kg; four male and four female animals per group). Serial blood samples (approximately 0.2 mL; taken at 0, 5, 15, 30 min, and 1, 1.5, 2, 4, 6, 8, 11, and 24 h) were directly collected from the orbital sinus under light ether anesthesia into heparinized polypropylene tubes containing 1 mg of BNPP. After gently shaking for 5–10 s, the blood samples were centrifuged at 1300×*g* for 10 min to yield plasma samples, which were kept frozen at -70 °C until analysis.

The tissue distribution of L-P was determined following iv administration (7.5 mg/kg, three male and three female rats per sampling time point, via the tail vein). Rats were euthanized by bleeding the abdominal aorta (approximately 10 mL of blood) at 0, 0.5, 2, 4, and 8 h. The blood samples were collected into heparinized polypropylene tubes that contained BNPP, followed by centrifugation to yield the plasma samples for analysis. Tissue samples of bladder, testicle (male only), ovary (female only), uterus (female only), stomach, small intestine, large intestine, spleen, kidney, liver, heart, lung, pancreas, adipose tissue, brain, skeletal muscle and femoral bones (and marrow) were excised and rinsed in ice-cold saline/methanol (1:1, *v/v*) before gentle blotting on absorbent paper and weighing. Most tissues were homogenized in 4 volumes of ice-cold saline/methanol (1:1, *v/v*). The tissues of the pancreas, adipose tissue and ovaries were prepared in 9 volumes of the ice-cold saline/methanol. The bladder tissue was prepared in 19 volumes of ice-cold saline/methanol. The homogenates were stored at -70 °C.

For urinary and fecal excretion studies, rats (three male and three female) were housed individually in Nalgene metabolic cages (Nalgene Co, Rochester, NY, USA) and received an iv dose of L-P at 7.5 mg/kg (via the tail vein). Urine and feces samples were collected predose and at 0 to 4, 4 to 10, 10 to 24, 24 to 34, and 34 to 48 h postdose. The urine and feces collection tubes were frozen at -15 °C to keep the collected samples

stable. All of the excretory samples were weighed before storage at -70 °C. The thawed feces samples were homogenized in 9 volumes of saline for analysis.

Rats were anesthetized with ether, and the bile duct was cannulated using polyethylene tubing. Bile was collected predose and at 0 to 0.5, 0.5 to 1, 1 to 2, 2 to 3, 3 to 6, 6 to 9, and 9 to 12 h after an iv dose of L-P at 7.5 mg/kg (three male and three female rats per sampling segment, administration via the tail vein). The bile samples were weighed and stored at -70 °C before use.

Tumor-bearing nude mice studies

The tissue distributions of L-P and L-2-Z were investigated in tumor-bearing nude mice. Mice were randomly assigned to five groups and received a single iv bolus dose of L-P at 15 mg/kg (via the tail vein; 3 mL/kg; four male and four female mice per group). After dosage, the mice under ether anesthesia were euthanized by bleeding the abdominal aorta (approximately 1 mL of blood) at 0, 0.25, 1, 2, 4, and 8 h (one group of mice was used for each time point). The blood samples were collected according to the same procedure used for the rats and were centrifuged to yield the plasma samples for analysis. Samples of the heart, liver, lung, kidney, pancreas, colon and tumors were excised and rinsed in ice-cold saline/methanol (1:1, *v/v*) before gently blotting on absorbent paper and weighing. The tissues were homogenized in 4 (the liver, kidney, colon and tumors), 9 (the heart and lung) or 29 (the pancresas) volumes of the ice-cold saline/methanol. The homogenates were stored at -70 °C.

Dog studies

Dogs were randomly assigned to three dosage groups and received a single iv bolus dose of L-P at 1.25, 2.5, or 5 mg/kg (via the forelimb vein; 1 mL/kg; four male and four female animals per group). The formulation was the same as that described for rat and mouse studies. Serial blood samples (approximately 0.3 mL; 0, 5, 15, 30 min and 1, 1.5, 2, 3, 4, 6, 8, 11, and 24 h) were directly collected from the opposite forelimb vein into heparinized polypropylene tubes containing 1.5 mg of BNPP. After gently shaking for 5 to 10 s, the blood samples were centrifuged at 1300×*g* for 10 min to yield the plasma samples that were kept frozen at -70 °C until analysis.

Pharmacokinetic data analysis

Plasma concentration-time data were analyzed for the calculation of pharmacokinetic parameters with a non-compartmental model analysis using the Thermo Kinetica software package (version 5.0, InnaPhase Corp, Philadelphia, PA, USA). The maximum concentration (C_{max}) and the time taken to achieve the peak concentration (T_{max}) after iv dosing were obtained directly from the data without interpolation. The area under plasma concentration-time curve ($AUC_{0\to t}$) up to the last measured time point was calculated by the trapezoidal rule. The terminal elimination half-life ($t_{1/2}$) was calculated using the relationship 0.693/k. The total plasma clearance ($CL_{tot,p}$) for iv dosing was estimated by dividing the administered dose by the $AUC_{0\to t}$. The distribution volume at steady status (V_{SS}) for iv dosing was estimated by multiplying the $CL_{tot,p}$ by the mean residence time (MRT). Dose proportionality assessments of $AUC_{0\to t}$ and C_{max} data for iv administered L-P in rats were conducted by the regression of the log-transformed data (the Power Model)[4]. The correlation coefficient (r^2), slope, and 90% confidence intervals for the slope were calculated, and inferences were made based on a theoretical slope of 1 and confidence limits of 0.84 to 1.16. All results were expressed as the arithmetic mean plus standard deviation.

Protein binding analysis

The binding of L-P and L-2-Z to plasma proteins of the rats, beagle dogs and humans was determined *in vitro* using a high-speed, rapid ultrafiltration method, as described previously[5]. In brief, Microcon YM-30 centrifugal filter devices (*g*-force <14 000 *g*, Millipore, Bedford, MA, USA) were used, and the plasma sample was spiked with L-P at 167, 836, and 3344 nmol/L, or L-2-Z at 248 and 1237 nmol/L. BNPP was added to the rat plasma (but not to dog and human plasma) before incubation, thus avoiding L-P conversion. The nonspecific binding of L-P and L-2-Z to the ultrafiltration membrane was also checked by filter-tested compounds in phosphate buffered saline (PBS, pH 7.4) using the same ultrafiltration devices. The nonspecific binding correction was made to calculate the protein binding (Equation 1) according to the literature[6].

$$PB(\%)=(1-\frac{C_{PF}\times C_{SD}}{C_{PD}\times C_{SF}})\times 100\%$$

where C_{PF} is the drug concentration in the plasma filtrate, C_{PD} is the measured plasma donor concentration, C_{SF} is the drug concentration in the PBS filtrate, and C_{SD} is the donor concentration measured in PBS before ultrafiltration.

In vitro assessment of inhibitory effects on cytochrome P450 enzymes

To evaluate the potential drug-drug interaction capabilities of L-P and its active metabolite L-2-Z, the inhibitory effects of L-P and L-2-Z on CYP1A2, CYP2C9, CYP2C19, CYP2D6, and CYP3A4 activities were examined using BD Gentest CYP inhibitor screening kits according to the manufacturer's instructions. The positive controls (inhibitors of enzyme activity) included furafylline for CYP1A2, sulfaphenazole for CYP2C9, tranylcypromine for CYP2C19, quinidine for CYP2D6, and ketoconazole for CYP3A4. L-P and L-2-Z were assessed, using recombinant CYPs, with respect to their capacity to inhibit the formation of fluorescent metabolites in reactions. These included 3-cyano-7-ethoxycoumarin → 3-cyano-7-hydroxycoumarin mediated by CYP1A2 or CYP2C19, 7-methoxy-4-trifluoromethylcoumarin → 7-hydroxy-4-trifluoromethyl coumarin by CYP2C9, 3-[2-(*N*,*N*-diethyl-*N*-methylamino)ethyl]-7-methoxy-4-methylcoumarin →3-[2-(*N*,*N*-diethylamino)ethyl]-7-hydroxy-4-methylcoumarin by CYP2D6, and 7-benzyloxy-trifluoromethylcoumarin → 7-hydroxy-4-trifluoromethyl coumarin by CYP3A4. Eight concentrations of L-P and L-2-Z or the positive controls were tested in two indepen-

dent experiments. For fluorescence intensity assays using a SpectraMax M2 Multi-Detection Reader (Molecular Devices, Sunnyvale, CA, USA), the metabolites were measured at selected excitation/emission wavelengths, *ie*, 410/460 nm for 3-cyano-7-hydroxycoumarin, 409/530 nm for 7-hydroxytrifluoromethyl coumarin, and 390/460 nm for 3-[2-(*N*,*N*-diethylamino) ethyl]-7-hydroxy-4-methylcoumarin. The half-maximal inhibitory concentration (IC_{50}) of the test compound was calculated from the concentration of the tested compound and the corresponding percent inhibition via linear interpolation. The inhibitory potency towards the CYP enzymes was classified as potent (IC_{50}<1 μmol/L), moderate (1 μmol/L<IC_{50}<10 μmol/L), weak (IC_{50}>10 μmol/L), or no inhibition (IC_{50}>100 μmol/L).

In vitro L-P activation assays by liver microsomal carboxylesterases of different species

The *in vitro* conversion of L-P to L-2-Z by liver microsomal carboxylesterase in different species was accomplished using 2 mg of total protein in a final volume of 200 μL of 100 mmol/L Tris-HCl buffer (pH 7.4) containing 5 μmol/L L-P. The reactions were incubated at 37 °C for 18 h and terminated by the addition of 500 μL cold acidified methanol. Reaction mixtures were centrifuged at 16 060×*g* for 10 min, the supernatant (5 μL) was applied to liquid chromatography/tandem mass spectrometry (LC-MS-MS) analysis.

Liquid chromatography/tandem mass spectrometry-based quantification of L-P and L-2-Z in various biological samples

In our previous study, an accurate analytical method was developed for the determination of L-P and L-2-Z in various plasma samples, based on the immediate deactivation of blood carboxylesterases activities by its inhibitor BNPP after blood sampling[7]. This well-validated bioanalytical method was applied to the preclinical pharmacokinetic research of L-P and L-2-Z. The biological samples (30 μL) were mixed with 10 μL of 100 ng/mL internal standard solution and extracted with 90 μL of acetonitrile (including 0.5% of formic acid). The acidified acetonitrile solution converted carboxylate L-P and L-2-Z into their lactone forms, and the total concentrations of L-P and L-2-Z were measured. After centrifugation at 16 060×*g* for 10 min, the supernatant (5 μL) was applied to LC-MS-MS analysis.

LC-MS-MS system was assembled from a Waters Acquity UPLC separation module (Milford, MA, USA) and an AB Sciex API 4000 Q Trap mass spectrometer (Toronto, Canada) with Turbo V ESI-source.

Chromatographic separation was achieved on a 5-μm Agilent ZORBAX Eclipse Plus C18 column (50 mm×2.1 mm ID; Santa Clara, CA, USA) at ambient temperature. The mobile phases were acetonitrile/water, 1:99 (*v*/*v*), containing 10 mmol/L formic acid, for A and acetonitrile/water, 99:1 (*v*/*v*), modified with the same electrolyte, for B. A pulse gradient chromatographic method was used. In brief, the gradient parameters, including the start proportion, start proportion segment, elution proportion, elution proportion segment, and column equilibrium segment, were 4% B, 0.5 min, 100% B, 2.5 min, and 1 min, respectively.

The ESI-MS-MS parameters were optimized to maximize the generation of the singly protonated species and to produce the characteristic product ions for the test compounds and internal standards. The precursors to the product ion pairs used for the multiple reaction monitoring of L-P, L-2-Z, irinotecan, and camptothecin were *m/z* 599→124, 405→361, 587→195, and 349→305, respectively. The LC eluent was introduced to the ESI source at a flow rate of 0.40 mL/min for data acquisition over the period of 1.4 to 2.0 min.

Matrix-matched calibration curves were constructed for L-P and L-2-Z using weighted (1/X) linear regressions of the analyte/IS peak area ratio (Y) against the corresponding nominal plasma concentrations of the analytes (X, nmol/L). The blank plasma samples were treated with BNPP to deactivate the carboxylesterases before use.

Liquid chromatography/tandem mass spectrometry-based metabolite profiling of L-P in various rat samples

The biological samples for metabolite profiling analyses included those of plasma, urine, bile and feces from male rats that received an iv dose of L-P at 7.5 mg/kg in the preceding plasma pharmacokinetic and excretion studies. An aliquot of 30 μL of the biological samples was extracted with 90 μL of acidic acetonitrile. After centrifugation, the supernatant was injected onto an LC-MS system for metabolite profiling. The mobile phase for metabolite profiling was the same as that used for the quantification of L-P and L-2-Z, with the flow rate set at 1.0 mL/min (0.5 mL/min of the LC eluent was introduced into the ESI source). Chromatographic separation was achieved on a 5-μm Agilent ZORBAX Eclipse DB C18 column (150 mm×4.6 mm ID) at ambient temperature. A gradient program was used with the following parameters: start proportion (10% B), start proportion segment (5 min), elution proportion (70% B), elution proportion segment (12 min), and column equilibrium segment (3 min). Metabolite profiling of L-P in the rat samples was conducted using full-scan ESI-interfaced LC–MS in both the positive- and negative-ion modes, according to the molecular mass gains or losses predicted for the possible metabolites compared with those of the parent compound. The metabolite prediction was performed according to the list of the common biotransformations of drugs[8] and was facilitated by the PALLAS MetabolExpert 3.7 software (CompuDrug International, Sedona, AZ, USA). The metabolites were characterized by LC-MS-MS at the collision energy 30 V in the full scan ranging from *m/z* 50 to *m/z* 1000. To compare the abundance (peak area) of the detected metabolites of L-P (M1-M9) in the preceding rat samples, the selective ion monitoring values of *m/z* 599, 405, 581, 631, 615, 571, and 587 were monitored for L-P, M1, M2, M3, M4, M5, M6, M7, M8, and M9, respectively. In addition, the abundance value for the excretory sample was further corrected with the volume of urine or bile of the sampling time interval or the mass of feces of the sampling time interval.

Results

Plasma pharmacokinetics in rats

The plasma pharmacokinetic parameters of L-P and its active metabolite L-2-Z after an iv bolus administration to rats are summarized in Table 1. After the iv dosing, L-P was eliminated from plasma with a mean $t_{1/2}$ of approximately 1.4 h (Figure 1), which was dose independent. The mean $CL_{tot,\,p}$ of L-P was observed to range from 1.52 to 1.82 $L{\cdot}h^{-1}{\cdot}kg^{-1}$ at three doses. Meanwhile, the mean V_{SS} of L-P (2.86–3.34 L/kg) was approximately 5-fold greater than the average volume of rat total body water (0.67 L/kg)[9], suggesting that L-P could be extensively distributed to the tissues. The biotransformation of L-P to its active metabolite L-2-Z after dosage was very fast: the mean T_{max} values of L-2-Z were 0.08–0.14 h at three doses. The systemic exposure ratio of L-P to L-2-Z ($AUC_{L\text{-}P}/AUC_{L\text{-}2\text{-}Z}$) ranged from 9.23 to 16.4 for the dosages tested. The elimination half-lives of L-2-Z at different doses (2.12–2.25 h) were relatively longer than those observed for the parent drug. The $AUC_{0\to24\ h}$ and C_{max} of plasma L-P and L-2-Z increased as the iv doses increased from 3.75 to 15 mg/kg, while the dose proportionality of the $AUC_{0\to24\ h}$ and C_{max} were not conclusively linear (Table 2). No gender difference was observed for the calculated pharmacokinetic parameters.

Tissue distribution in rats

The results of the tissue distribution examinations for L-P and L-2-Z in rats 30 min, 2, 4 and 8 h after the iv administration of L-P are summarized in Figure 2. L-P and L-2-Z were rapidly

Table 1. Plasma pharmacokinetic parameters (mean±SD) of L-P and L-2-Z in tumor-bearing nude mice, rats and dogs receiving iv bolus doses of L-P.

PK parameters	L-P Nude mice (*n*=8) 15 mg/kg			L-2-Z Nude mice (*n*=8) 15 mg/kg		
C_{max} (nmol/L)	5142±658			2726±872		
T_{max} (h)	–			0.44±0.3		
$AUC_{0\to24\ h}$ (nmol/L·h)	8142±1398			5405±1722		
$t_{1/2}$ (h)	0.95±0.1			1.45±0.1		
MRT (h)	1.14±0.1			1.96±0.3		
$CL_{tot,\,p}$ ($L{\cdot}h^{-1}{\cdot}kg^{-1}$)	3.16±0.6			–		
V_{ss} (L/kg)	3.57±0.6			–		
$AUC_{L\text{-}P}/AUC_{L\text{-}2\text{-}Z}$	1.51			–		
PK parameters[a]	Rat (*n*=8)					
	L-P			L-2-Z		
	3.75 mg/kg	7.5 mg/kg	15 mg/kg	3.75 mg/kg	7.5 mg/kg	15 mg/kg
C_{max} (nmol/L)	1651±344	3518±285	7191±626	299±129	307±51	469±62
T_{max} (h)	–	–	–	0.08±0.0	0.10±0.1	0.14±0.2
$AUC_{0\to24\ h}$ (nmol/L·h)	3709±434	8922±1796	17906±2794	402±73	652±131	1093±219
$t_{1/2}$ (h)	1.45±0.1	1.46±0.1	1.42±0.1	2.20±0.3	2.25±0.2	2.12±0.1
MRT (h)	1.85±0.1	1.92±0.2	1.91±0.2	2.65±0.7	3.12±0.3	2.97±0.2
$CL_{tot,p}$ ($L{\cdot}h^{-1}{\cdot}kg^{-1}$)	1.82±0.2	1.54±0.3	1.52±0.3	–	–	–
V_{ss} (L/kg)	3.34±0.3	2.91±0.4	2.86±0.3	–	–	–
$AUC_{L\text{-}P}/AUC_{L\text{-}2\text{-}Z}$	9.23	13.7	16.4	–	–	–
PK parameters	Dog (*n*=6)					
	L-P			L-2-Z		
	1.25 mg/kg	2.5 mg/kg	5 mg/kg	1.25 mg/kg	2.5 mg/kg	5 mg/kg
C_{max} (nmol/L)	616±62	1135±126	2101±319	13.9±2.3	25.1±4.6	43.2±4.9
T_{max} (h)	–	–	–	0.58±0.2	0.46±0.1	0.5±0.0
$AUC_{0\to24\ h}$ (nmol/L·h)	2050±446	3712±514	6417±1718	41.6±5.9	69.6±8.3	106±19
$t_{1/2}$ (h)	1.95±0.1	1.90±0.2	1.72±0.1	2.20±0.5	2.23±0.5	1.73±0.3
MRT (h)	2.74±0.3	2.74±0.2	2.45±0.2	3.25±0.6	3.16±0.6	2.53±0.2
$CL_{tot,p}$ ($L{\cdot}h^{-1}{\cdot}kg^{-1}$)	1.12±0.2	1.20±0.2	1.46±0.3	–	–	–
V_{ss} (L/kg)	3.03±0.4	3.27±0.3	3.54±0.7	–	–	–
$AUC_{L\text{-}P}/AUC_{L\text{-}2\text{-}Z}$	49.3	53.3	58.6	–	–	–

[a] C_{max}, peak plasma concentration, the results of L-P were those of $C_{5\ min}$; T_{max}, time to reach peak plasma concentration; $AUC_{0\to24\ h}$, area under the concentration-time curve from zero up to 24 h; $t_{1/2}$, half-life of elimination phase; MRT, mean residence time; $CL_{tot,p}$, total plasma clearance; V_{ss}, distribution volume at steady status.

Table 2. Dose proportionality assessment of $AUC_{0\to 24\ h}$ and C_{max} in rats and dogs receiving an iv dose of L-P.

Compound	Systemic exposure parameter	r^2	Slope (90% CI)	Conclusion[a]
Rat (dosage: 3.75, 7.5, and 15 mg/kg)				
L-P	$AUC_{0\to 24\ h}$	0.938	1.135 (1.003, 1.267)	Inconclusive
	C_{max}	0.957	1.073 (0.970, 1.176)	Inconclusive
L-2-Z	$AUC_{0\to 24\ h}$	0.834	0.721 (0.601, 0.842)	Inconclusive
	C_{max}	0.409	0.362 (0.164, 0.560)	Nonlinear
Beagle dog (dosage: 1.25, 2.5, and 5.0 mg/kg)				
L-P	$AUC_{0\to 24\ h}$	0.856	0.818 (0.640, 0.996)	Inconclusive
	C_{max}	0.954	0.882 (0.779, 0.984)	Inconclusive
L-2-Z	$AUC_{0\to 24\ h}$	0.889	0.677 (0.550, 0.804)	Nonlinear
	C_{max}	0.906	0.823 (0.683, 0.963)	Inconclusive

[a] The term "linear" was concluded if the 90% confidence interval (CI) for slope was contained completely within the reference interval of dose proportionality criterion (0.84–1.16); "inconclusive" was concluded if the 90% CI lay partly within the reference interval; "nonlinear" was concluded if the 90% CI was entirely outside the reference interval.

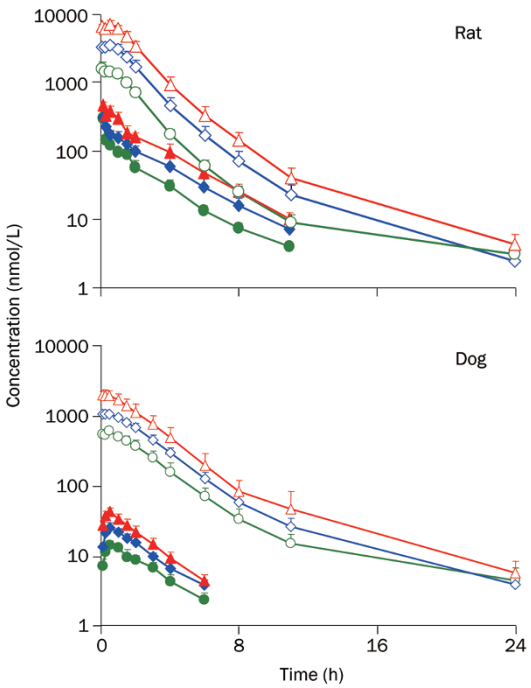

Figure 1. Plasma concentration-time profiles of L-P and the metabolite L-2-Z in rats (upper panel) and beagle dogs (lower panel) receiving an iv bolus dose of L-P. △, ◇, and ○ represents L-P plasma levels at 15, 7.5, and 3.75 mg/kg doses to rats and 5.0, 2.5, and 1.25 mg/kg to dogs, respectively. ▲, ◆, and ● represents L-2-Z plasma levels in rats and dogs at corresponding doses of L-P. Time schedule for blood sampling in rats and in beagles were 0, 5, 15, 30 min, 1, 1.5, 2, 3 (for beagles only), 4, 6, 8, 11, and 24 h after dosing. Data are expressed as the mean and standard deviation from 8 animals (four males and four females).

distributed to tissues of the rats. The highest concentrations of L-P in all tested tissues were observed 30 min after dosing. Most of the tissues (except for the brain, testicle, and adipose) had significantly higher concentrations of L-P than those observed in the plasma. The highest concentrations of L-P were found in rat pancreas, kidney, and liver 30 min after dosing. These data indicated that L-P was well distributed in rat tissues, which is consistent with the preceding plasma V_{SS} data. L-2-Z was found to be distributed in most of the tissues, with the exception of the brain. The highest concentrations of L-2-Z in all tested tissues were observed 30 min after dosing, which resembled the distribution of the parent compound. The concentrations of L-2-Z in liver, kidney and small intestine were higher than that observed in the plasma.

Urinary, biliary and fecal excretion in rats

The results of the excretion experiments in rats indicated that after the iv administration of L-P at 7.5 mg/kg to rats, 13% of the administered dose was excreted in urine as L-P (0.32 μmol), and 1.3% was excreted as L-2-Z (0.03 μmol). Most of the L-P (90%) and L-2-Z (70%) were excreted within the first 4 h after dosing. Meanwhile, more than 95% of the L-P and 80% of L-2-Z were excreted into the bile within 6 h after dosing. Approximately 51% of the administered dose was recovered [48% as L-P (1.20 μmol) and 3.0% as L-2-Z (0.08 μmol)] in the bile and urine; biliary excretion was the predominant route of L-P excretion. These results are consistent with the tissue distribution studies, in which L-P and L-2-Z were found to have high concentrations in the liver and kidney. Moreover, the recovery of the administered dose from feces was 19% (0.48 μmol) as L-P and 12% (0.29 μmol) as L-2-Z over the first 48 h, which had a lower amount of L-P and a higher amount of L-2-Z than the amounts of these compounds excreted in bile. Figure 3 depicts the cumulative amount of L-P and L-2-Z excreted from urine, bile and feces, as well as the corresponding percentage of the dose recovered from excretory samples in rats.

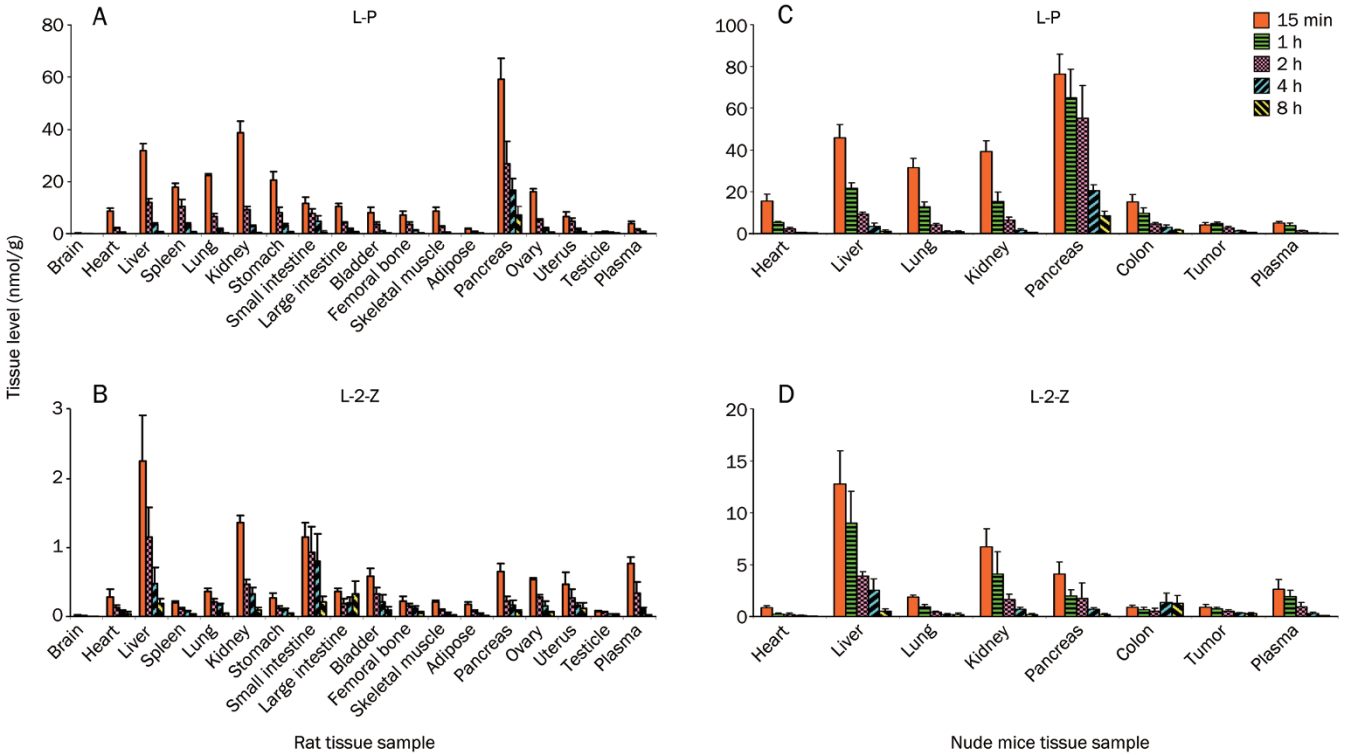

Figure 2. Tissue distribution profile of L-P (A) and L-2-Z (B) in rats and L-P (C) and L-2-Z (D) in nude mice receiving an iv bolus dose of L-P at 7.5 mg/kg and 15 mg/kg, respectively. Data are expressed as mean±SD from 6 rats (three males and three females) and 8 mice (four males and four females).

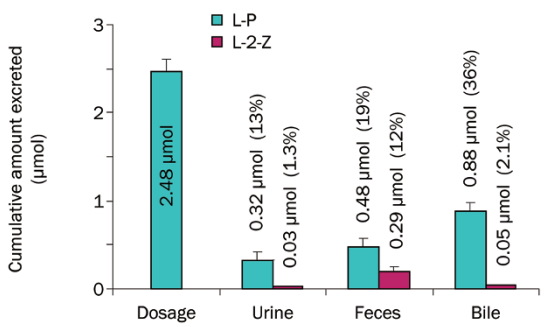

Figure 3. Cumulative amount of L-P and L-2-Z excreted from urine, bile and feces, and percentage of dose recovered from excretory samples of rats (n=6, three males and three females) receiving an iv bolus dose of L-P at 7.5 mg/kg. Data are expressed as mean±SD of cumulative amounts in μmol/L.

Metabolic profile in rats

Metabolic profiling assays revealed the occurrence of nine L-P metabolites (M1–M9) in bile, seven metabolites (M1–M7) in urine and five (M1–M3, M6, M7) in rat plasma following the iv administration of L-P at 7.5 mg/kg. The detection and collision induced dissociation (CID) data on these metabolites are summarized in Table 3, and Figure 4 depicts the proposed metabolic pathways. No metabolites were detected in the biofluids from the untreated rats. The MS–MS analysis of the metabolites indicated that M1 was the active metabolite of L-2-Z, M2 was the phase II glucuronide conjugate of M1, M3–M7 were phase I oxidative metabolites of L-P, and M8 was a decarboxylation product of L-P that could be further oxidized to form M9.

Compared with the abundance of plasma L-P from the iv-administered L-P, M1 was the major plasma metabolite, with a plasma metabolite-to-parent compound ratio in $AUC_{0\to 24\ h}$ ($AUC_M/AUC_{L\text{-}P}$) of 0.045. M2, M3, M6, and M7 were demonstrated to be minor plasma metabolites whose $AUC_M/AUC_{L\text{-}P}$ values ranged from 0.001 to 0.008. These plasma metabolites were also measured in the rat urine and bile samples. M4 and M5 were found in urine and bile, but not in plasma, while M8 and M9 were only found in bile. In addition, two metabolites (M2 and M4) were excreted in relatively large amounts compared to other metabolites. M2 exhibited $Cum.A_{e\ M}/Cum.A_{e\ L\text{-}P}$ values of 0.17 and 0.25 in urine and bile, respectively; and M4 had a $Cum.A_{e\ M}/Cum.A_{e\ L\text{-}P}$ value of 0.30 in bile. The sums of the individual $Cum.A_{e\ M}/Cum.A_{e\ L\text{-}P}$ (M2–M9) values were 0.4 and 0.9 in urine and bile, respectively. These results demonstrated that metabolism is also an important elimination route of iv-administered L-P.

Tissue distribution in tumor-bearing nude mice

After iv administration of L-P at 15 mg/kg to a nude mice xenograft model of human hepatic cancer SMMC-7721 cell line, L-P and L-2-Z distributed to the tissues rapidly. The highest concentrations of these two compounds were observed at 15 min after the dosage. In addition, L-P was measured at

Table 3. Parent ions (PI), fragment ions (FI), and LC retention times (t_R) of L-P metabolites, as well as the exposure data.

ID	PI[a] (*m/z*)	FI[b] (*m/z*)	t_R (min)	$AUC_m/AUC_{L\text{-}P}$[c]	*Cum.*$A_{e\,M}$/*Cum.*$A_{e\,L\text{-}P}$[d] Urine	Bile
L-P	599	415, 389, **167**, 124, 86, 84	9.2	1.00	1.00	1.00
M1(L-2-Z)	405	**361**, 305, 276, 275	10.4	0.045	0.059	0.037
M2	581	**405**, 361, 305	8.8	0.0011	0.17	0.25
M3	631	**613**, 587, 569, 195	8.6	0.0083	0.041	0.043
M4	631	613, 587, 569, **405**, 227, 209	9.0	–	0.051	0.30
M5	615	571, **553**, 541, 195	8.5	–	0.017	0.16
M6	615	597,**571**, 553, 211,183	8.8	0.014	0.046	0.11
M7	615	**597**, 571, 553, 195	9.0	0.0044	0.030	0.063
M8	571	**553**, 195,167	9.1	–	–	0.018
M9	587	543, **525**, 497, 469,195	8.1	–	–	0.018

[a] $[M+H]^+$ generated in the positive ion ESI mode.
[b] Produced from the $[M+H]^+$ by CID. The number in bold is for the base peak and the fragment ions of relative abundance <5% are not shown.
[c] $AUC_M/AUC_{L\text{-}P}$, plasma metabolite-to-L-P ratio in $AUC_{0\to 24\,h}$, which were calculated from the peak areas because of the reference standards of metabolites not available.
[d] *Cum.*$A_{e\,M}$/*Cum.*$A_{e\,L\text{-}P}$, cumulated amount excreted from urine or bile, which was calculated from the ratio of metabolite to parent compound.

significantly higher concentrations in pancreas, heart, liver, lung, and kidney than that in plasma after dosing. The tumor tissue and colon had comparable L-P levels to those of plasma (Figure 2). The measured L-2-Z levels in the tested tissues were lower than the L-P levels. The distribution of L-2-Z in the tumor tissues supports the results of the *in vivo* efficacy studies that reported a dramatic inhibition of tumor growth in several human tumor xenograft nude mice models[3].

Plasma pharmacokinetics in beagle dogs

Following iv dosing to beagle dogs, L-P was eliminated from plasma with mean $t_{1/2}$ values ranging from 1.72 to 1.95 h (Figure 1), L-P elimination was unaffected by dose and resembled the results obtained in rats. The mean $CL_{total,p}$ of L-P was observed to be 1.12–1.46 $L\cdot h^{-1}\cdot kg^{-1}$. Meanwhile, the mean V_{SS} of L-P (3.03–3.54 L/kg) was approximately 5-fold greater than the average volume of dog total body water (0.60 L/kg), suggesting that L-P could be extensively distributed to the tissues. The systemic exposure ratio of L-P to L-2-Z ($AUC_{L\text{-}P}/AUC_{L\text{-}2\text{-}Z}$) ranged from 49 to 59 in the dosages tested (Table 1). The $AUC_{0\to 24\,h}$ and C_{max} of plasma L-P and L-2-Z in dogs increased as the iv doses increased from 1.25 to 5 mg/kg, while the dose proportionality of $AUC_{0\to 24\,h}$ and C_{max} were not conclusively linear (Table 2).

Plasma protein binding in different species

The plasma protein bindings of L-P in rat, dog and human plasma were 59.9%–72.3%, 18.0%–24.2%, and 36.9%–39.9% in the range of 167–3344 nmol/L, respectively. The L-2-Z plasma protein binding in the above respective species was 77.0%–83.1%, 44.5%–53.6%, and 75.7%–86.0% in the range of 248–1237 nmol/L. The non-specific binding of L-P and L-2-Z to the filter membrane and plastic parts of the centrifugal filter device was approximately 24% and 27%, respectively, and was corrected in the protein binding calculation. Thus, L-P and L-2-Z showed low to moderate binding to plasma proteins, and L-2-Z bound stronger to plasma proteins than its prodrug L-P. Compared to the literature values of plasma protein binding for irinotecan and its active metabolite SN-38[10], the plasma protein binding of L-P and L-2-Z in humans is relatively lower. Furthermore, the active metabolites bind more strongly to plasma protein than their parent drugs due to their higher lipophilicity.

In vitro inhibitory effects on human CYP enzymes

As shown in Table 4, furafylline, sulfaphenazole, tranylcypromine, quinidine, and ketoconazole showed IC_{50} values of 1.45, 0.19, 4.50, 0.0057, and 0.028 μmol/L for cDNA-expressed CYP1A2, CYP2C9, CYP2C19, CYP2D6, and CYP3A4, respectively; these values are in agreement with the values provided by the manufacturer. L-P showed no inhibitory effect on the activity of CYP1A2, CYP2C9, and CYP2C19. It showed weak inhibitory effects on CYP2D6 (IC_{50} values of 32.9 μmol/L) and moderate inhibitory effects on CYP3A4 (IC_{50} values of 8.95 μmol/L). L-2-Z showed no inhibitory effect on the activity of CYP2D6, a weak inhibitory effect on CYP1A2, CYP2C9, and CYP2C19 (IC_{50} value of 43.7, 21.3, and 19.3 μmol/L, respectively), and a moderate inhibitory effect on CYP3A4 activity, with an IC_{50} value of 6.10 μmol/L.

In vitro biotransformation of L-P to L-2-Z by liver microsomal carboxylesterases of different species

The biotransformation of L-P to L-2-Z by liver microsomal carboxylesterases was determined by monitoring the stability of L-P and the formation of its active metabolite L-2-Z in liver microsomes of different species by LC-MS-MS. Liver microsomes of rats, dogs, monkeys and humans were incubated with 5 μmol/L of L-P at 37 °C for up to 18 h, and the concentrations of L-P and L-2-Z were measured. The results indicated that the $t_{1/2}$ of L-P in liver microsomes of rat, dog,

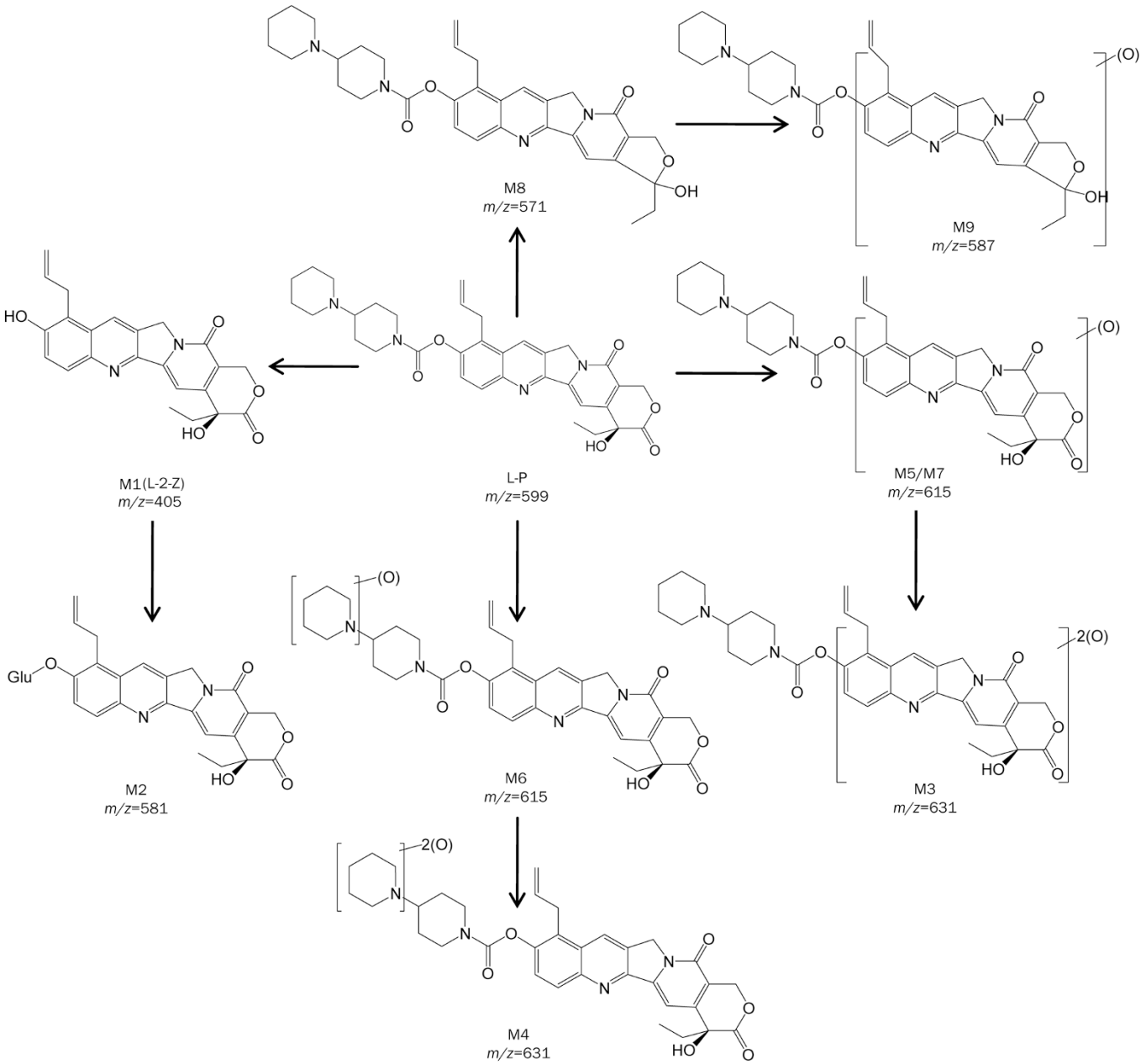

Figure 4. Proposed metabolic pathways of L-P in rats.

Table 4. *In vitro* inhibitory effects of L-P and L-2-Z on CYP enzymes.

Enzyme	Reaction	Control (positive inhibitor)	IC_{50} (μmol/L) L-P	L-2-Z
CYP1A2	CEC ⟶ CHC	1.45 (Furafylline)	No inhibition	43.7
CYP2C9	MFC ⟶ HFC	0.19 (Sulfaphenazole)	No inhibition	21.3
CYP2C19	CEC ⟶ CHC	4.50 (Tranylcypromine)	No inhibition	19.3
CYP2D6	AMMC ⟶ AMHC	0.0057 (Quinidine)	32.9	164
CYP3A4	BFC ⟶ HFC	0.028 (Ketoconazole)	8.95	6.10

CEC, 3-cyano-7-ethoxycoumarin; CHC, 3-cyano-7-hydroxycoumarin; MFC, 7-methoxy-4-trifluoromethylcoumarin; HFC, 7-hydroxytrifluoromethyl coumarin; AMMC, 3-[2-(*N*,*N*-diethyl-*N*-methylamino)ethyl]-7-methoxy-4-methylcoumarin; AMHC, 3-[2-(*N*,*N*-diethylamino)ethyl]-7-hydroxy-4-methylcoumarin; BFC, 7-benzyloxy-trifluoromethylcoumarin; HFC, 7-hydroxytrifluoromethylcoumarin.

monkey and human were 3.82, 4.20, 3.77, and 3.37 h, respectively. The formation of L-2-Z was 4.08, 0.40, 11.3, and 9.41 $nmol \cdot h^{-1} \cdot mg^{-1}$ protein, respectively, in the above species. Compared to the stability of L-P and the formation of L-2-Z in the plasma of mice, rats, dogs and humans[7], L-P was unstable and the formation of L-2-Z was approximately 2000 to 4000 $nmol \cdot mL^{-1} \cdot h^{-1}$ in rodents, while L-P was stable and L-2-Z could not be detected in the plasma of dogs and humans. These results suggest that in rodents, the biotransformation of L-P to its active metabolite L-2-Z predominantly occurs in the plasma rather than in the liver. In dogs and humans, however, due to the absence of carboxylesterase activity in plasma, hepatic carboxylesterases-mediated biotransformation of L-P to L-2-Z played an important role in the antitumor activities of L-P.

Discussion

The delivery of drugs with limited water solubility remains a challenge in drug development. The prodrug strategy is an older but time-tested approach, which utilizes bioreversible and more water-soluble derivatives of the problematic molecule. The stable, bioreversible and quantitative release of the active drug moiety is required for prodrug modifications. Irinotecan, the first-line antineoplastic agent, is an analog of L-P and is a successful prodrug that has improved aqueous properties for parenteral administration[11, 12]. The use of irinotecan over SN-38 is also due to the beneficial steady-state kinetics obtained in the use of the prodrug form[13]. Irinotecan has an ethyl substituent at position 7 and a dipiperidyl carbamate at position 10, which is metabolized to SN-38 and is 100 to 1000 times more cytotoxic than the prodrug[14]. Its structure and biotransformation are very similar to that of L-P. In this study, we report preclinical pharmacokinetics and metabolism studies on L-P and its active metabolite L-2-Z, including the *in vivo* ADME properties following iv dosage to rodent and non-rodent species as well as its *in vitro* metabolism in liver microsomes of different species and an assessment of its inhibitory effects on cytochrome P450 enzymes. These studies led to the projection of human efficacious concentrations and doses and enabled an assessment of the potential for drug-drug interactions with concomitantly administered drugs.

Following iv administration, L-P and L-2-Z exhibited relatively short elimination half-lives in rats and dogs. The clearance of L-P in nude mice ($3.2\ L \cdot h^{-1} \cdot kg^{-1}$) was larger than that observed in rats ($1.6\ L \cdot h^{-1} \cdot kg^{-1}$) and dogs ($1.3\ L \cdot h^{-1} \cdot kg^{-1}$). The volume of distribution in rats and dogs was greater than total body water, indicating extensive extravascular distribution. The plasma protein binding of L-P and L-2-Z was measured to be moderate (≤81.6%) in plasma of different species. SN-38 was found to have a high level of plasma protein binding, *ie*, 94%–96%, in the concentration range of 50–200 ng/mL in human[10]. The tested compounds showed relatively lower plasma protein binding than their camptothecin analogs.

The prodrug L-P is biotransformed to its active metabolite L-2-Z in rats, mice and beagle dogs after iv administration. In this study, significant species differences were observed among the examined animals, in which rodents showed a much higher conversion ratio than dogs. The $AUC_{L\text{-}P}/AUC_{L\text{-}2\text{-}Z}$ values ranged from 9.23 to 16.4 in rats (3.75–15 mg/kg), 1.51 in nude mice (15 mg/kg), and 49.3 to 58.6 in dogs (1.25–5 mg/kg). Carboxylesterases are responsible for the conversion of L-P to L-2-Z[7] and the activities of carboxylesterases in rodents, dogs and humans are different. High activities of carboxylesterases were observed in the plasma, liver and intestine of rodents, while only low activity was found in the liver and intestines of dogs. For primates, moderate carboxylesterases activity could be observed in the liver and intestines[15]. Our results are consistent with the reported enzyme activities in different species. The conversion of irinotecan to SN-38 through cleavage of the ester-bond at C10 was shown to be catalyzed by two human isozymes of liver carboxylesterases, *ie*, hCE-1 and hCE-2[16, 17]. Due to the structural similarity of L-P to irinotecan, these two isozymes most likely play an important role in L-P conversion in cancer patients.

In the tissue distribution experiment, L-P and L-2-Z were observed to have high concentrations in rat liver and kidney. This finding was consistent with the excretion results showing that the prodrug and its metabolite were excreted mainly from bile. L-P and L-2-Z distributed to the rat brain with low concentrations. The K_p ($AUC_{brain,free}/AUC_{plasma,free}$) ratios were 0.20 and 0.16 for L-P and L-2-Z, respectively. Various studies reported that central nervous system toxicity is associated with administration of irinotecan[18] and that the mechanism could be explained by electron transfer functionalities and oxidative stress generated from reactive oxygen species to the central nervous system[19]. Accordingly, neurotoxicity induced by L-P and/or L-2-Z should also be monitored during clinical antitumor therapy.

Tissue distribution results obtained in tumor-bearing nude mice indicated that L-P was measured at higher levels in pancreas, liver and kidney, which is consistent with the results obtained from the rats. Furthermore, in the tissue distribution studies in rats and nude mice, the levels of L-P were found to be highest in the pancreas at all time points investigated. Due to the weak anticancer activity of L-P *in vitro*, it is unlikely to exhibit any significant therapeutic benefit for pancreatic disease. However, the toxic side effects caused by this compound in the pancreas should be closely monitored. In the case of L-2-Z, the tissue accumulative concentrations in mice were relatively higher than those in rats, in which a similar distribution order exists. In this study, we found that the carboxylesterase-mediated hydrolysis of L-P to L-2-Z is more significant in mice than in other species. The $AUC_{L\text{-}P}/AUC_{L\text{-}2\text{-}Z}$ value was 1.51 in nude mice (15 mg/kg) (Table 1), indicating a much higher biotransformation than that observed in rats (9.23–16.4) and dogs (49.3–58.6). The systemic higher exposure of L-2-Z caused higher tissue distribution levels in nude mice. In addition, the higher conversion of L-P to its active metabolite L-2-Z could explain the higher total plasma clearance of L-P in nude mice ($3.2\ L \cdot h^{-1} \cdot kg^{-1}$) than in rats ($1.6\ L \cdot h^{-1} \cdot kg^{-1}$). It has been reported that carboxylesterases are highly expressed in human neuroblastoma cell lines[20]. The presence of tumors increased

the systemic exposure of SN-38 after the iv or *po* administration of irinotecan in mice bearing human neuroblastoma xenografts[21]. In the present study, however, the nude mice bearing hepatocellular carcinoma cell lines may not express carboxylesterases activities; therefore, the L-2-Z measured in tumor tissues was possibly derived from the circulation.

The results of the excretion experiments indicated that L-P is mainly eliminated via biliary excretion. An interesting phenomenon we observed was that L-P and L-2-Z were recovered in bile accounting for 36% and 2.1%, respectively, of the administered dose. However, L-P was only recovered 19% of the administered dose in the feces, and L-2-Z was found to be recovered at a higher amount (12%) in feces than that in the bile (2.1%). Considering that rat intestine is also an organ with high carboxylesterase activity[15], it is possible that biliary excreted L-P will undergo biotransformation to its active metabolite L-2-Z in the intestine, which could result in further excretion in the feces. Additionally, the β-glucuronidase derived from enterobacteria may be responsible for the hydrolysis of L-2-Z glucuronide (M2) to form the active L-2-Z. In the metabolite profiling of L-P in current study, we detected a large amount of M2 in rat bile ($Cum.A_{e\,M}/Cum.A_{e\,L\text{-}P}$=0.25), which also supports this hypothesis. Furthermore, L-2-Z produced in the intestine could be reabsorbed into the systemic circulation, which is consistent with SN-38[13, 22]. Enterohepatic recirculation may prolong the terminal elimination half-life of drugs[23], which might interpretate the relatively longer elimination half life of L-2-Z than that of the prodrug in the current study.

Our *in vitro* data indicated that L-P and L-2-Z showed a moderate inhibitory effect on CYP3A4 (IC_{50} values of 8.95 and 6.10 μmol/L, respectively). Caution should thus be exercised during the examination of the potential of a drug-drug interaction mediated by the inhibitory effects of L-P and L-2-Z on CYP3A4 in clinical use.

In summary, L-P, a water-solubility ameliorated prodrug, can be biotransformed to its active metabolite L-2-Z inside animals' bodies, and it quantitatively released the active drug moiety in response to the doses investigated. The elimination half-lives of iv-administered L-P and its metabolite L-2-Z were relatively short. L-P and L-2-Z rapidly and extensively distribute to rat and mice tissues. Biliary excretion is the predominant route of L-P in rats. Nonetheless, species differences in carboxylesterase activities caused a significant disparity in the biotransformation of the prodrug L-P to its active metabolite L-2-Z in rodents, beagle dogs and humans. These differences should be considered when designing dose escalation protocols as well as to prevent possible gastrointestinal toxicity induced by L-2-Z in clinical studies.

Acknowledgements

This work was supported by the National Science & Technology Major Project of China "Key New Drug Creation and Manufacturing Program" (Grant No 2009ZX09304-002, 2009ZX09301-001 and 2009ZX09102-020), the National Natural Science Foundation of China (Grant No 30873120) and the Chinese National Natural Science Foundation for Distinguished Young Scholars (Grant No 30925044). The authors would like to thank Dr Jian DING and Dr Ze-hong MIAO from the Shanghai Institute of Materia Medica for their assistance.

References

1 Rivory L, Haaz M, Canal P, Lokiec F, Armand J, Robert J. Pharmacokinetic interrelationships of irinotecan (CPT-11) and its three major plasma metabolites in patients enrolled in phase I/II trials. Clin Cancer Res 1997; 3: 1261–6.
2 Haas N, LaCreta F, Walczak J, Hudes G, Brennan J, Ozols R, *et al*. Phase I/pharmacokinetic study of topotecan by 24-h continuous infusion weekly. Cancer Res 1994; 54: 1220–6.
3 Huang M, Gao H, Chen Y, Zhu H, Cai Y, Zhang X, *et al*. Chimmitecan, a novel 9-substituted camptothecin, with improved anticancer pharmacologic profiles *in vitro* and *in vivo*. Clin Cancer Res 2007; 13: 1298–307.
4 Smith BP, Vandenhende FR, DeSante KA, Farid NA, Welch PA, Callaghan JT, *et al*. Confidence interval criteria for assessment of dose proportionality. Pharm Res 2000; 17: 1278–83.
5 Guo B, Li C, Wang GJ, Chen LS. Rapid and direct measurement of free concentrations of highly protein-bound fluoxetine and its metabolite norfluoxetine in plasma. Rapid Commun Mass Spectrom 2006; 20: 39–47.
6 Lee KJ, Mower R, Hollenbeck T, Castelo J, Johnson N, Gordon P, *et al*. Modulation of nonspecific binding in ultrafiltration protein binding studies. Pharm Res 2003; 20: 1015–21.
7 Hu Z, Sun Y, Du F, Niu W, Xu F, Huang Y, *et al*. Accurate determination of the anticancer prodrug simmitecan and its active metabolite chimmitecan in various plasma samples based on immediate deactivation of blood carboxylesterases. J Chromatogr A 2011; 1218: 6646–53.
8 Kostiainen R, Kotiaho T, Kuuranne T, Auriola S. Liquid chromatography/atmospheric pressure ionization-mass spectrometry in drug metabolism studies. J Mass Spectrom 2003; 38: 357–72.
9 Davies B, Morris T. Physiological parameters in laboratory animals and humans. Pharm Res 1993; 10: 1093–5.
10 Combes O, Barre'J, Duche'J, Vernillet L, Archimbaud Y, Marietta M, *et al*. *In vitro* binding and partitioning of irinotecan (CPT-11) and its metabolite, SN-38, in human blood. Investig New Drugs 2000; 18: 1–5.
11 Rautio J, Kumpulainen H, Heimbach T, Oliyai R, Oh D, Jarvinen Y, *et al*. Prodrugs: design and clinical applications. Nat Rev 2008; 7: 255–70.
12 Stella V, Nti-addae K. Prodrug strategies to overcome poor water solubility. Adv Drug Deliv Rev 2007; 59: 677–94.
13 Kaneda N, Nagata H, Furuta T, Yokokura T. Metabolism and pharmacokinetics of the camptothecin analogue CPT-11 in the mouse. Cancer Res 1990; 50: 1715–20.
14 Hertzberg R, Caranfa M, Holden K, Jakas D, Gallagher G, Mattern M, *et al*. Modification of the hydroxy lactone ring of camptothecin: inhibition of mammalian topoisomerase I and biological activity. J Med Chem 1989; 32: 715–20.
15 Berry L, Wollenberg L, Zhao Z. Esterase activities in the blood, liver and intestine of several preclinical species and humans. Drug Metab Lett 2009; 3: 70–7.
16 Slatter J, Su P, Sams J, Schaaf L, Wienkers L. Bioactivation of the anticancer agent CPT-11 to SN-38 by human hepatic microsomal carboxylesterases and the *in vitro* assessment of potential drug interactions. Drug Metab Dispos 1997; 25: 1157–64.

17 Humerickhouse R, Lohrbach K, Li L, Bosron W, Dolan M. Characterization of CPT-11 hydrolysis by human liver carboxylesterase isoforms hCE-1 and hCE-2. Cancer Res 2000; 60: 1189–92.
18 Hamberg P, Donders R, ten Bokkel Huinink D. Central nervous system toxicity induced by irinotecan. J Natl Cancer Inst 2006; 98: 219.
19 Kovacic P. Mechanism of central nervous system toxicity by irinotecan. Med Hypotheses 2006; 67: 997.
20 Ehrich M, Veronesi B. Esterase comparison in neuroblastoma cells of human and rodent origin. Clin Exp Pharmacol Physiol 1995; 22: 328–86.
21 Zamboni WC, Houghton PJ, Thompson J. Altered irinotecan and SN-38 disposition after intravenous and oral administration of irinotecan in mice bearing human neuroblastoma xenografts. Clin Cancer Res 1998; 4: 455–62.
22 Takeda Y, Kobayashi K, Akiyama Y, Soma T, Handa S, Kudoh S, *et al*. Prevention of irinotecan (CPT-11)-induced diarrhea by oral alkalization combined with control of defecation in cancer patients. Int J Cancer 2001; 92: 269–75.
23 Marier J, Vachon P, Gritsas A, Zhang J, Moreau J, Ducharme M. Metabolism and disposition of resveratrol in rats: extent of absorption, glucuronidation, and enterohepatic recirculation evidenced by a linked-rat model. J Pharmacol Exp Ther 2002; 302: 369–73.